

Normalized Cut with Reinforcement Learning in Constrained Action Space

Qize Jiang
qzjiang21@m.fudan.edu.cn
FuDan University
China

Linsey Pang
panglinsey@gmail.com
Salesforce
USA

Alice Gatti
alicegatti1992@gmail.com
Center for AI Safety
USA

Mahima Aggarwal
maggarwal@hbku.edu.qa
Qatar Computing Research Institute, HBKU
Qatar

Giovanna Vantini
gvantini@hbku.edu.qa
Qatar Computing Research Institute, HBKU
Qatar

Xiaosong Ma
Xiaosong.Ma@mbzuai.ac.ae
Mohamed bin Zayed University
United Arab Emirates

Weiwei Sun
wwsun@fudan.edu.cn
FuDan University
China

Sanjay Chawla
schawla@hbku.edu.qa
Qatar Computing Research Institute, HBKU
Qatar

Abstract

Reinforcement Learning (RL) has emerged as an important paradigm to solve combinatorial optimization problems primarily due to its ability to learn heuristics that can generalize across problem instances. However, integrating external knowledge that will steer combinatorial optimization problem solutions towards domain appropriate outcomes remains an extremely challenging task. In this paper, we propose the first RL solution that uses constrained action spaces to guide the normalized cut problem towards pre-defined template instances. Using transportation networks as an example domain, we create a Wedge and Ring Transformer that results in graph partitions that are shaped in form of Wedges and Rings and which are likely to be closer to natural optimal partitions. However, our approach is general as it is based on principles that can be generalized to other domains.

1 Introduction

Reinforcement Learning (RL) has emerged as a powerful heuristic for tackling complex combinatorial optimization

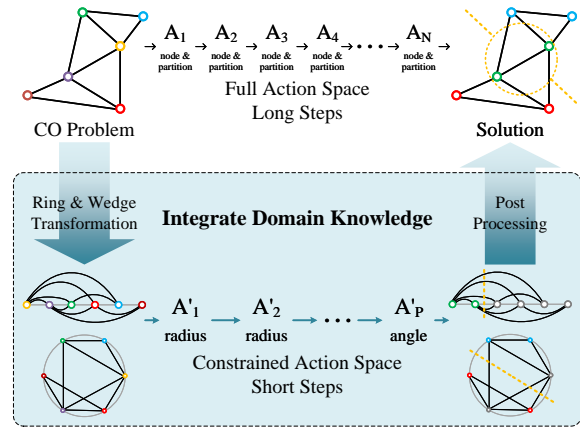


Figure 1: Finding better solution by integrating domain knowledge and learning in the constrained action space. Take Graph Partitioning as example.

tion (CO) problems [15, 39, 27]. Two key insights underpin the use of RL in CO: first, the search space of CO can be encoded into a vector embedding; second, gradients can be computed even when the objective is a black-box function or non-differentiable. A significant advantage of RL frameworks is that once trained, they can solve new instances of

CO problems without starting from scratch [10].

When addressing real-world problems through combinatorial optimization, utilizing insights from the specific domain can lead to improved performance compared with standard CO problems. However, integrating this domain knowledge into reinforcement learning poses significant challenges. Existing methods often fail to leverage domain knowledge effectively. Typically, this knowledge is incorporated by either augmenting states or modifying rewards [31, 26, 18]; however, these approaches do not fully adhere to the instructions provided by the domain knowledge, and they may result in suboptimal performance. To address this issue, we propose a novel approach that employs a constrained action space informed by domain knowledge. By adopting this method, agents can prioritize the exploration of more pertinent actions, thereby accelerating training and learning more effective strategies.

In this paper, we address a specific problem to demonstrate the effectiveness of constraining the action space in RL for CO problems. Our primary focus is on the Normalized Cut (NC) of a graph, which is suitable to balance the simulating traffic on road networks. Figure 1 illustrates the proposed direction of our work. Existing RL methods for solving graph partitioning problems typically involve the direct movement of adjacent nodes between partitions. These approaches have full action space, but often require a long or potentially unlimited number of steps to achieve optimal partitions. In contrast, our method integrates domain knowledge pertaining to ring and wedge partitioning. By constraining the action space to the partition radius and angle, we significantly reduce the necessary number of steps, and resulting in improved partitioning outcomes.

The ring and wedge configuration represents a fundamental structure in modern urban cities. Road networks are often organized as concentric rings of roads centered at a city downtown followed by wedge structures connecting the outer ring. For example, Beijing’s Five Ring includes a large circular expressway encircling the city, acting as the outermost “ring” within the urban area, while traffic flows from various surrounding suburban areas converge toward the city center. Moreover, at the end of major events, individuals typically expand outward from the center of the stadium, exhibiting a radial dispersion through the main avenues. For microscopic traffic simulation, where the movement of every vehicle is modeled in a simulator, it often becomes necessary to partition the road network and assign each partition to a separate simulator in order to reduce the overall simulation time. We thus ensure that the partitions respect the natural physical topology of the road network, and this understanding serves as a vital domain knowledge when conducting graph partitioning on road networks. Directly using classical approaches like METIS, spectral clustering or modern Graph Neural Networks (GNN) based RL

solutions provide no provision to constrain the generation of partition shapes justifying the need for a new approach.

To integrate domain knowledge and thereby constrain the action space, our key insight is to convert complex graph structures into simpler representations, such as a line or a circle, and reducing the complexity of the partitioning problem. In the ring transformation, nodes are projected onto the x -axis according to their radial distance from the center, preserving the node order and partitioning properties. Similarly, in the wedge transformation, nodes are projected onto a unit circle, focusing on their angular positions. These transformations allow us to apply Transformers [37], which can scale more effectively to large graphs compared to traditional GNNs, allowing us to better constrain the action space after the transformation. With this approach, instead of moving nodes to adjacent partition sequentially, we can directly select the radius and angle for ring and wedge partitions.

After transforming the graph, we apply Proximal Policy Optimization (PPO)[34] to solve the partitioning problem. Our approach leverages the ability of Transformers to capture both local interactions and global patterns across the entire graph. We demonstrate that our method outperforms existing RL-based and traditional methods, particularly in handling weighted planar graphs. In addition to optimizing Normalized Cut, we explicitly measure the *ringness* and *wedgeness* of the generated partitions. We give performance visualization in Figure 2. In Figure 2(a), a snapshot of the partitions generated by different methods shows that other methods except our proposed method WRT tend to mix nodes from different partitions, resulting in high Normalized Cut. Figures 2(b) and 2(c) introduce Ringness and Wedgeness metrics to evaluate how closely a partition aligns with ring and wedge structures. Our proposed method, WRT, achieves the lowest Normalized Cut while maintaining the highest Ringness and Wedgeness scores.

Our main contributions are as follows:

- Propose a novel direction to integrate domain knowledge into reinforcement learning by constraining the action space.
- introduce the ring-wedge partitioning scheme WRT, which simplifies graph structures to effectively support constrained action space.
- Develop a novel RL-based approach to minimize Normalized Cut on planar weighted graphs, and implementing two-stage training process which improves partitioning performance and stability.
- Conduct extensive experiments on synthetic and real-world graphs, demonstrating that our algorithm has superior performance and scales to graphs with varying sizes effectively.

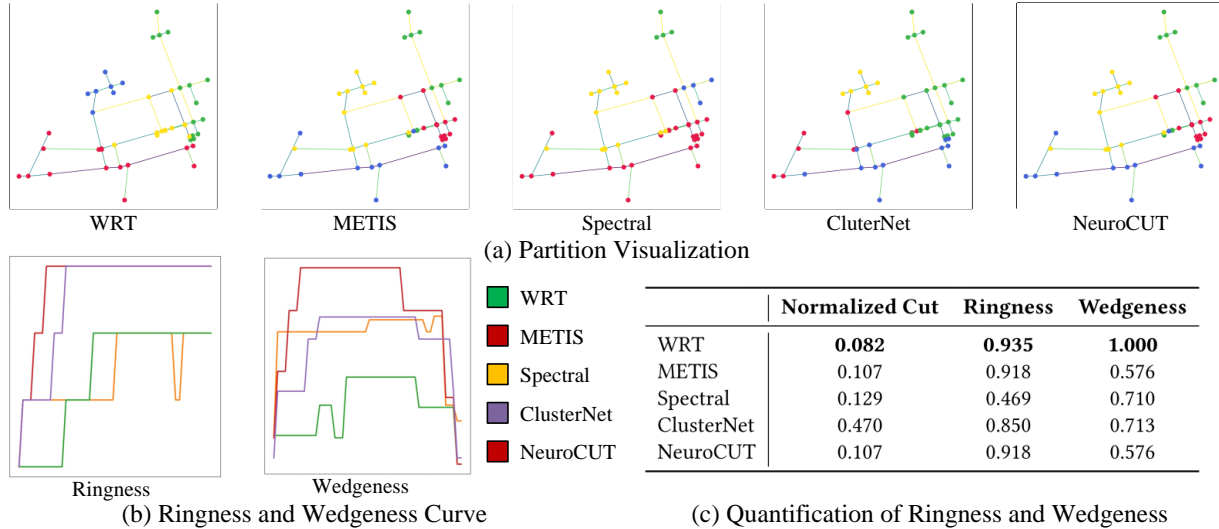


Figure 2: Compared with other methods, WRT has the minimal Normalized Cut, and also achieves the highest Ringness and Wedgeness. NeuroCUT is initialized by METIS partition, and fails to find a better one, which causes the same result.

2 Related Work and Preliminaries

2.1 Graph Partitioning

Graph partitioning [6] is widely used in graph-related applications, especially for enabling parallel or distributed graph processing. Partitioning a graph into k blocks of equal size while minimizing cuts is NP-complete [17]. Exact methods focus on bipartitioning [16] or few partitions ($k \leq 4$) [11], while approximate algorithms include spectral partitioning [29, 9] and graph-growing techniques [14]. More powerful methods involve iterative refinement, such as node-swapping for bipartitioning [23], extendable to k -way local search [21]. Other approaches include the bubble framework [8] and diffusion-based methods [28, 30]. State-of-the-art techniques rely on multilevel partitioning [22], which coarsen the graph and refine the partition iteratively.

The most well-known tool are METIS [1, 22], which uses multilevel recursive bisection and k -way algorithms, with parallel support via ParMetis [2] and hypergraph support via hMetis [19, 20]. Other tools include Scotch [3, 30] and KaHIP [33] use various advanced techniques. However, these methods fail to give optimal partitions with normalized cuts, and are also unable to integrate extra domain knowledge.

2.2 ML-based Graph Partitioning Algorithms

Recent research has explored machine learning methods for graph partitioning, particularly using GNN [24, 38, 5]. GNN aggregate node and edge features via message passing. In [12], a spectral method is proposed where one

GNN approximates eigenvectors of the graph Laplacian, which are then used by another GNN for partitioning. The RL-based method in [13] refines partitions in a multilevel scheme. NeuroCUT [35] introduces a reinforcement learning framework that generalizes across various partitioning objectives using GNN. It demonstrates flexibility for different objectives and unseen partition numbers. ClusterNet [40] integrates graph learning and optimization with a differentiable k -means clustering layer, simplifying optimization tasks like community detection and facility location. However, neither of these methods handles weighted graphs, making them unsuitable in our scenarios.

Although GNN excel at aggregating multi-hop neighbor features, they struggle to globally aggregate features without information loss, which is critical for combinatorial problems like graph partitioning. Our work addresses these limitations by constraining the action space of reinforcement learning agents with domain knowledge, which is unable for existing GNN-based methods. Specifically, we introduce graph transformation methods and applying Transformer to learn global features.

2.3 Reinforcement Learning

In our work, we use Reinforcement Learning, specifically PPO to train the model with non-differential optimizing targets. Proximal Policy Optimization (PPO) [34] is a widely-used RL algorithm that optimizes the policy by minimizing a clipped surrogate objective, ensuring limited deviation from the old policy π_{old} . The PPO objective maximizes $\mathbb{E}_t [\min(r_t(\theta)A_t, \text{clip}(r_t(\theta), 1 - \epsilon, 1 + \epsilon)A_t)]$, where $r_t(\theta) = \frac{\pi_\theta(a_t|s_t)}{\pi_{\theta_{\text{old}}}(a_t|s_t)}$ and A_t is the advantage.

3 Problem Description

Let $G = (V, E, W, o)$ be a weighted planar graph, with vertex set V , edge set E , edge weights W , and a predefined center o . A k -way partition P of G is defined as a partition $\{p_1, \dots, p_k\}$ of V , where $\bigcup_{i=1}^k p_i = V$ and $\forall i \neq j, p_i \cap p_j = \emptyset$. The definition of the **Normalized Cut** is as follows: For each partition p_i , we define

$$Cut(G, p_i) = \sum_{u \in p_i \otimes v \in p_j} W(e_{u,v}) \quad (1)$$

$$Volume(G, p_i) = \sum_{u,v \in p_i} W(e_{u,v}) + Cut(G, p_i), \quad (2)$$

where \otimes represents the XOR operator. The *normalized cut* of a partition P on graph G is then defined as

$$NC(G, P) = \max_{i \in \{1..k\}} \frac{Cut(G, p_i)}{Volume(G, p_i)}. \quad (3)$$

We aim to find partitions that minimize the normalized cut, a known NP-complete problem, and thus we focus on approximate solutions. The goal is to learn a mapping function $f_\theta(G) = P$ that minimizes $NC(G, P)$.

To perform a better partition strategy, we utilize the domain knowledge that performing ring and wedge partition on road networks are efficient, so we restrict our attention to partitions with specific structures, where each partition is either ring-shaped or wedge-shaped. We also allow for "fuzzy" rings and wedges, where a small number of nodes are swapped to adjacent partitions. This relaxation helps achieve partitions with a smaller normalized cut, particularly for graphs derived from real-world applications.

Our partitioning strategy follows a three-step process: first, we perform a ring partition on the entire graph, then we apply a wedge partition to the outermost rings, and finally, we refine the resulting partitions to further reduce the normalized cut. Figure 3 illustrates these three steps.

Ring Partition: A Ring Partition of the graph G with respect to the center o , denoted by P^r , divides G into k_r distinct concentric rings. Define the radii as $0 = r_0 \leq r_1 \leq r_2 \leq \dots \leq r_{k_r-1} < r_{k_r}$. These radii partition G into k_r rings, where the i -th ring, denoted as p_i^r , contains all nodes with a distance to the center o between r_{i-1} and r_i .

Wedge Partition: A Wedge Partition, denoted as P^w , divides the outermost ring $p_{k_r}^r$ into multiple wedge-shaped sections. The partitioning angles are given by $0 \leq a_1 \leq a_2 \leq \dots \leq a_{k_w} < 2\pi$. These angles split $p_{k_r}^r$ into k_w wedge parts, where the i -th wedge, p_i^w , contains the nodes whose polar angles are between $[a_i, a_{i+1})$, except for the wedge $p_{k_w}^w$, which contains nodes whose angles fall within either $[0, a_1)$ or $[a_{k_w}, 2\pi)$.

This type of partition divides the graph into $k_r - 1$ inner rings and k_w wedges on the outermost ring (see Figure 3). Specifically, if $k_r = 1$, the entire graph is partitioned solely by wedges and, conversely, if $k_w = 1$ the graph is partitioned solely by rings. For simplicity, when a graph G is partitioned by a Ring-Wedge Partition with k_r and k_w , we define $k = k_r + k_w - 1$, with $p_k = p_k^r$ when $k < k_r$, and $p_k = p_{k-k_r+1}^w$ when $k \geq k_r$. And we define the total partition strategy as $P = \{p_1, \dots, p_k\}$.

We also propose the Ringness and Wedgeness to evaluate whether a partition is close to the ring shape or wedge shape. The definition of Ringness and Wedgeness can be found in the Appendix.

Besides the practical aspects, partitions structured as a combination of ring and wedge subsets is also theoretically well behaved. For a specific classes of graphs, they satisfy bounds similar to the ones that are satisfied by partitions achieving minimum normalized cut. In the next section, we provide these bounds for them.

4 Cheeger Bound for Ring and Wedge Partition

In the graph partitioning context there exists bounds on the Cheeger constant in terms of the normalized Laplacian eigenvalues, see for example [7] for bisection and [25] for more general k -partitions. Intuitively, the Cheeger constant measures the size of the minimal "bottleneck" of a graph and it is related to the optimal partition. Since we consider a subset of all the possible partition classes, namely ring and wedge, we show that the normalized cut defined in (3) satisfies bounds similar to the classical case in the case of unweighted spider web graphs. Despite being a simpler class of graphs, these bounds give a theoretical justification of the normalized cut definition (3) and the ring-wedge shaped partition. (see the proof in Appendix).

Definition: Let $G_{n,r}$ be an unweighted spider web graph with r rings and n points in each ring, and k be an integer. Define the wedge and ring Cheeger constants as:

$$\phi_{n,r}(k) = \min_{\substack{P=V_1 \cup \dots \cup V_k \\ \text{wedge partition}}} NC(G_{n,r}, P) \quad (4)$$

$$\psi_{n,r}(k) = \min_{\substack{P=V_1 \cup \dots \cup V_k \\ \text{ring partition}}} NC(G_{n,r}, P). \quad (5)$$

Proposition 1. Let $G_{n,r}$ be a spider web graph with r rings and N nodes in each ring. Let λ_k^C and λ_k^P be the eigenvalues of the circle and path graphs with n and r vertices respectively. Then

$$\phi_{n,r}(k) \leq \frac{2r}{2r-1} \sqrt{2\lambda_k^C}, \quad 2 \leq k \leq n \quad (6)$$

$$\psi_{n,r}(k) \leq \sqrt{2\lambda_k^P}, \quad 2 \leq k \leq r \quad (7)$$

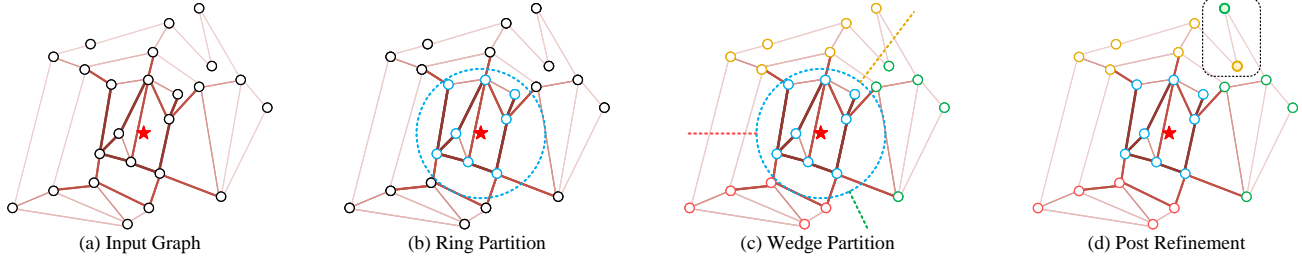


Figure 3: Graph partitioning with Ring and Wedge to minimize the Normalized Cut. We firstly do ring partitions as (b), to choose different radii to partition the graph into rings. Then for the out-most ring, we do partitions based on different angles as (c). Finally, we do post refinement to improve the final partition performance as (d).

5 Methodology

To elaborate on our approach, we begin by introducing the settings of reinforcement learning environment, then we provide a comprehensive overview of the agent’s function and its interactions with the environment to achieve the final partitioning. We then dive into the detailed structure of the proposed method. Finally, we discuss the training methodologies and the post refinement method designed to enhance performance.

For simplicity, we will pre-define the ring partition number k_r and wedge partition number k_w . When k -partitioning a graph, we will enumerate all possible ring partition numbers, then select the one that minimizes the Normalized Cut.

5.1 Reinforcement Learning Environment

We primarily employ reinforcement learning methods to address the ring-wedge partitioning problem. The observation space, action space and reward function are defined in the following. The agent’s final goal is to maximize the reward through interactions with the environment described above.

Observation Space The observation space S contains the full graph G , the expected ring number k_r , wedge number k_w , and the current partition P , denoted by $S = \{G, k_r, k_w, P\}$.

Action Space The agent needs to decide the next partition as action. If it is a Ring Partition, the action is the *radius* of next ring, if it is a Wedge Partition the action is the partition *angle* of the wedge.

$$A = \begin{cases} r & \text{if currently expects a ring partition} \\ a & \text{if currently expects a wedge partition} \end{cases}$$

Reward Function

When the partitioning process is incomplete, we assign a reward of 0. Conversely, when partitioning process is complete, the reward is thereby formulated as the negative of

the Normalized Cut, reflecting our objective to minimize this metric, i.e. $r = -NC(G, P)$.

5.2 Graph Transformation

In previous deep learning-based graph partitioning methods, most of them involved a combination of GNNs and RL. However, GNNs face limitations as they only aggregate the local structure of the graph, necessitating an initial partition followed by fine-tuning. This approach is inadequate for our application, as we require the model to produce ring and wedge partition results directly.

Recently, Transformers have achieved remarkable success across various domains, utilizing Multi-Head Attention to facilitate global information exchange, thus demonstrating superior performance in diverse tasks. For our specific problem, we aim for the model to learn the global view of the graph, leading us to naturally select the Transformer architecture. However, Transformers typically require sequential input, rendering them ill-suited for graph representations. To address this issue, we employ two transformations, Ring Transformation and Wedge Transformation, on the graph. These new representations maintain equivalence with the original graph for the purposes of Ring Partitioning or Wedge Partitioning, while re-organizing the data into a sequential format suitable for input into the Transformer.

5.2.1 Ring Transformation

Since the ring partition remains unchanged when rotating the graph around the center o , we can project each node onto the x -axis. More specifically, if a node has polar coordinates (r, θ) , the projection will map it to the coordinate $(r, 0)$. Figure 4 (b) illustrates this projection onto the line. We can observe that when the order of nodes on the line remains unchanged, we can adjust the radius of any point, and the partition results in the new graph will be identical to those in the original graph. By applying this conclusion, we can transform a standard graph into a simplified version

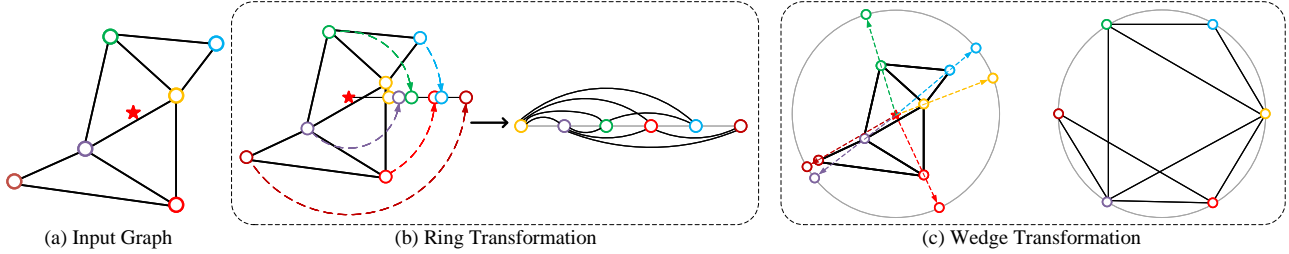


Figure 4: Example of Wedge Transform and Ring Transform. In Wedge Transform, nodes are projected to a circle, then the difference of angles of adjacent nodes are adjusted to the same. In Ring Transform, nodes are projected to a line. The edge connections and their weights are not changed in both transformation.

where every node is represented by the coordinates $(X, 0)$, where X is the radius order of the node among all nodes. This transformation does not alter the order of the nodes or the existing partitions. The result of this transformation is displayed on the right side of Figure 3 (b).

5.2.2 Wedge Transformation

Similar to Ring Transformation, we observe that during wedge partition, the radius of nodes does not influence the outcome; only the angle of the nodes is taken into account. We project all nodes onto a unit circle centered at point o . Thus, if the polar coordinates of a node are (r, X) , its corresponding projection will have coordinates $(1, X)$. After implementing the projection, we also modify the angles of the nodes. If a node's angle order is X among N nodes, its new polar coordinate will be adjusted to $(1, \frac{2\pi X}{N})$. This transformation process is illustrated in Figure 4 (c).

Following the transformation, nodes of the graph are positioned either along a line or on a circle, allowing us to treat the graph as a sequential input. Additionally, actions that split nodes i and $i + 1$ into two partitions yield identical final partition results. Consequently, we can convert the continuous action space into discrete actions to mitigate learning difficulties. A new action A_i indicates the partitioning of nodes i and $i + 1$ into two separate partitions.

5.3 Ring Wedge Partition Pipeline

The graph partition pipeline of the Wedge Ring Transformer (WRT) is illustrated in Figure 5 (a). It sequentially determines partitions through Ring and Wedge Transformations, iteratively predicting the next ring radius or wedge angle until the target partition count is achieved. The model consists of two components for ring and wedge partitions, sharing similar structures but distinct weights, and it contains four sub-modules.

Transformation: The appropriate transformation (ring or wedge) is applied based on current requirements.

Pre-Calculation: Essential computations on the transformed graph include: (1) Cut Weight C_i : Sum of edge weights crossing between nodes i and $i + 1$. (2) Volume Matrix $V_{i,j}$: Total weight of edges covered between nodes i and j (where $i < j$).

Wedge Ring Transformer: The Transformer processes node embeddings derived from the pre-calculation phase and the current partition status, as depicted in Figure 5 (b). A detailed discussion of its details will be provided in the subsequent subsection, and its detail will be discussed in the next subsection.

PPO Header: After receiving node embeddings, the PPO header extracts action probabilities and critic values. The actor projection header maps hidden size h to dimension 1, followed by a Softmax layer for action probabilities. Value prediction uses Self-Attention average pooling on node embeddings and projects from h to 1.

The model will perform one action with one forward, and is employed to execute actions recursively until the graph is fully partitioned. Also, during the Ring Partition phase, a dynamic programming algorithm calculates the optimal partition when the maximum radius and total ring count are fixed, with a complexity of $O(n^2k)$. Thus, the WRT determines the maximum radius for all ring partitions only once. The pseudo-code is available in the Appendix.

5.4 Wedge Ring Transformer (WRT)

WRT utilizes a Transformer backbone to leverage information from transformed graphs, enabling it to handle varying node counts and enhancing its scalability for diverse applications without the need for fine-tuning after training. The Transformer architecture is illustrated in Figure 5 (b).

WRT processes inputs from the Pre-Calculation module, specifically Cut Weight and Volume Matrix, along with the Current Partition from the input graph. These are fed into n Transformer blocks, yielding node embeddings from the final hidden state. To effectively manage Current Partition, we represent each node's selection status Partition Selection with a 0-1 array, then it is combined with Cut Weight and

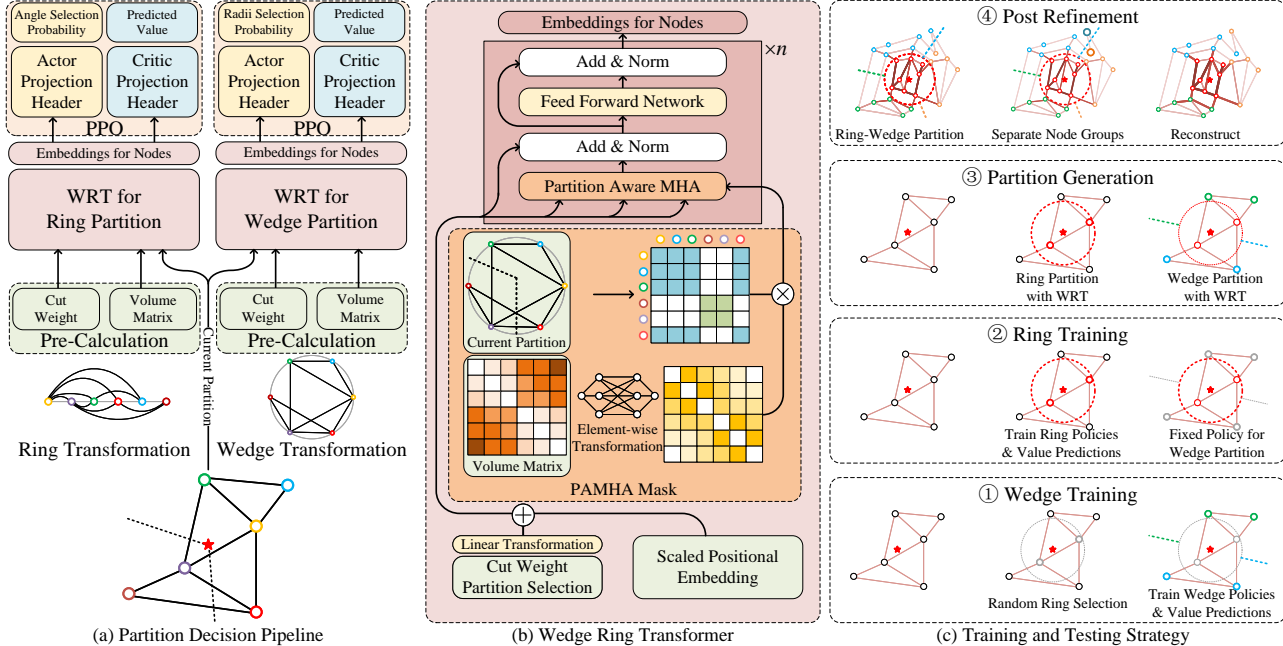


Figure 5: Framework and stages of the Wedge-Ring Transformer (WRT). (a) WRT first applies Ring and Wedge Transformations, followed by pre-calculation to obtain Cut Weight and Volume Matrix. The processed data generates node embeddings for action probabilities and predicted values via actor and critic projection headers. Modules for ring and wedge partition share structures but differ in weights. (b) Detailed structure of WRT, using cut weights with positional embeddings as input, followed by transformer layers. Partition Aware MHA Mask is used, which considers Volume Matrix and Current Partition to generate appropriate masks. (c) WRT pipeline from training to testing. Initially, the wedge partition strategy is trained with a random approach for the ring partition, then the wedge part is fixed while training the ring part, excluding its critic projection header. In testing, WRT sequentially determines ring radius and wedge angle, and refining the final partition using post-refinement.

transformed through a linear layer to generate hidden states, which are subsequently augmented with positional embeddings.

In WRT, we introduce Partition Aware Multi-Head Attention (PAMHA) to replace the original Multi-Head Attention (MHA) layer. PAMHA incorporates the Volume Matrix and Current Partition into its attention mask. An element-wise transformation on V produces an attention mask of shape $N \times N$ for PAMHA, allowing the model to learn the significance of different nodes. For Current Partition, we observe that partitions splitting between nodes i and $i + 1$ do not affect the normalized cut calculations on the right of $i + 1$. For instance, in the circular graph with six nodes depicted in Figure 5, two wedge partition angles are already established. When partitions are made among the red, green, blue, and yellow nodes, these modifications have no impact on the contributions from the brown and purple nodes. Consequently, we create an attention mask focusing solely on the effective range of nodes. Finally, WRT outputs node embeddings, which are then input to the PPO module.

5.5 Training and Testing Strategies

We employ specialized training and testing strategies to enhance policy learning and improve partition results. Both the training and testing processes are divided into two stages. A visualization of these four stages is depicted in Figure 5 (c).

5.5.1 Training Strategy

In previous model designs, WRT has effectively extracted information from graphs. However in RL, the initial strategies are inherently randomized, presenting a significant challenge in learning an optimal strategy. Specifically, the ring partition and wedge partition can interfere with one another. For instance, if the ring partition consistently selects the smallest radius as its action, the wedge partition will struggle to learn any valid policy. This occurs because in such situation, the Normalized Cut for the ring partition is considerably large, and the final Normalized Cut is significantly influenced by the ring partition, regardless of the actions taken by the wedge partition. Consequently, training

a ring partition with a low-quality wedge partition strategy will also encounter similar difficulties.

To mitigate the aforementioned problem, we have divided the policy training into two distinct stages, as illustrated in Figure 5 (c) ① and ②. In the first Wedge Training stage, we implement a randomized ring selection method to replace ring selection strategies in WRT. In this phase, WRT is only responsible for determining and optimizing the wedge partitioning. To enhance the model’s concentration on developing an effective wedge partition strategy, we intentionally ignored the Normalized Cut of ring partitions when evaluating the reward received by WRT. This approach ensures that the model is concentrated on mastering a robust wedge partitioning strategy.

In the second Ring Training stage, we allow WRT to determine both the ring and wedge partitions. However, we have observed that permitting the model to adjust its parameters related to wedge partitioning can lead to a decline in its ability to effectively execute wedge partitioning before it has fully developed an optimal strategy for ring partitioning. To mitigate this issue, we freeze the parameters of the wedge partitioning modules in WRT, because WRT has already established a robust wedge partitioning strategy across various radii. The only exception is the Critic Projection Header. In the previous stage, we modified this header to solely utilize the Normalized Cut of wedge partitions as the reward, which is inconsistent with current reward definition. Hence, during the Ring Training stage, both Critic Projection Headers are re-initialized and subsequently trained. In PPO, since the strategies are only determined by actor model, allowing the critic to be trainable does not interfere with the learned policy.

5.5.2 Testing Strategy

After WRT is fully trained, it can generate partitions directly during the Partition Generation stage. Initially, the model will perform a ring partition, followed sequentially by wedge partitions, as illustrated in Figure 5 (c) ③.

While we have proved that ring and wedge partitions possess similar upper bounds under certain constraints, in real-world graphs, these partitions may not yield optimal results when outliers exist. As illustrated in Figure 5 (c) ④, the original grouping of two nodes are reversed during the execution of a pure ring and wedge partition. To mitigate this problem, we propose a Post Refinement Stage, where nodes within the same partition that are not directly connected will be separated into distinct partitions. We then adopt a greedy approach to select the partition with the highest Normalized Cut, subsequently merging it with adjacent partitions. This post-refinement technique effectively reduces the number of outlier nodes and enhances the quality of the resulting partitions.

Finally, since PPO is a policy-gradient based method that generates an action probability distribution, relying on a single segmentation may not directly lead to the optimal solution. Therefore, we can perform multiple random samplings to obtain different partitions and select the best of them.

6 Experiments and Results

To demonstrate the superior performance of WRT, which integrates the domain knowledge that performing ring and wedge partition, we evaluate our model using both synthetic and real-world graphs, compared with other graph-partitioning methods. We firstly introduce the dataset details, then give the competitors in graph partitioning, and finally show the overall performance and ablation studies results.

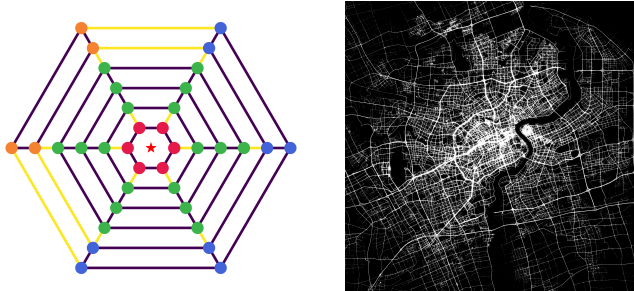
6.1 Graph Datasets

To make precise evaluation of different methods, we construct three types of graph datasets. The detailed definitions are in the following:

Predefined-weight Graph: In this dataset, we design the structure to resemble a spider web, which consists of N concentric circles, each having M equally spaced nodes. The radii of circles are from 1 to N . Given an unweighted spider web graph, built by randomly choosing the number of circles and the number of nodes, we also randomly select a valid ring-wedge partition configuration, specifying both the number of rings and wedges, and randomly performing such partitions. We then assign lower weights to edges that cross different partitions and higher weights to edges within the same partition (intra-partition edges). An example of synthetic spider web graph is given in Figure Figure 6a. More details about the ranges of nodes, circles, weights etc, for generating the graphs are included in Appendix.

Random-weight Graph: The graph structure is the same as above, but edge weights are assigned randomly in a given range. In the random-weight graphs, models should find best partition without prior knowledge. The statistics of our training and test synthetic graphs are shown in Table 5.

Real City Traffic Graph: For real-world data, we utilize sub-graphs randomly extracted from a comprehensive city traffic map (Figure 6b). The extracted sub-graph is always connected. For edge weights, we collect traffic data of the city during a specific time range to assess our method’s ability to handle real traffic volumes effectively. The statistical information of Real City Traffic Graph can be found in Table 5.



(a) Synthetic graph: 6 circles and 6 nodes on circle. Yellow edges is lower weights, other is higher weights. Current partition 2 rings and 2 wedges.

(b) City Traffic Map: Overview of a real traffic map. We randomly sample connected sub-graphs for training and testing.

Figure 6: Sample graphs used in experiments.

6.2 Models and Compared Methods

We compare our proposed method with the following baselines and methods.

For traditional approaches, we select: **METIS** solver that is used to partitioning graphs with balanced size. **Spectral Clustering** uses eigenvectors and k-means to perform graph partitioning.

We also propose two baselines for ring and wedge partitions: **Bruteforce** method to enumerate possible ring and wedge partitions. **Random** to randomly generate 10,000 partitions and choose the best performance one as the result.

For Reinforcement Learning based graph partitioning methods, we select two state-of-the-art methods, **ClusterNet** and **NeuroCUT**, which are introduced in Subsection 2.2.

Finally, we compare above methods with our proposed WRT. We also compare these methods with the variants of WRT, and the results are in the Appendix due to the space limitation.

6.3 Performance Evaluation

6.3.1 Evaluation of Model Overall Performance

We show the overall performance in Table 1. We tested our model in three different types of datasets described in Section 6.1 and summarized in Table 5, with 4 or 6 partition numbers. The number of graphs used for training is 400,000. We test the performance of different methods on 100 randomly generated graphs and report the average performance. We can find that our method always performs best compared with other methods on all datasets, showing its superior performance compared with existing methods, with the reduced ring-wedge shaped action space. Although

Metis and Spectral Clustering can give graph partitions with any shape, they still cannot reach better performance compared with our proposed methods, because it is hard to find best results in such huge action space. Two basic methods, Bruteforce and Random, although they follow the ring and wedge partition, their performances are always worst compared with other methods, because they do not consider the differences of edge weights, and only do random partitioning.

6.3.2 Evaluation of Model Transfer Performance

We train the model on three types of graphs, each containing a fixed number of nodes ($N=100$) within each circle. Then we conduct transfer learning experiments on graphs with node counts $N=50$ and $N=200$ without fine-tuning. The results presented in Table 2 demonstrate that our model exhibits significant generalizability. When trained on graphs of a specific size, it effectively applies to graphs of other sizes.

6.3.3 Ringness and Wedgeness Evaluation

Ringness and Wedgeness are quantitative indicators used to evaluate the proximity of a partition to Ring and Wedge partitions, from ring and wedge viewpoint respectively. The detailed definitions of Ringness and Wedgeness are provided in Appendix D. Table 3 presents the quantification results of Ringness and Wedgeness across City Traffic Graphs. It is noteworthy that the WRT method achieves the highest levels of them when compared to other approaches.

6.3.4 Inference Time Evaluation

We provide inference time of our method and other competitors on City Traffic graphs with 4 partitions in the table 4. We can observe that METIS and ClusterNet have relatively low and stable running time; Spectral Clustering, while also having a shorter running time in the experiments, exhibits a rapid increase based on node number. NeuroCUT, takes a longer time and shows a significant growth as the number of points increases. Our method WRT takes relatively longer than METIS and ClusterNet, but is significantly faster than NeuroCUT.

7 Conclusion and Future Work

In this paper, we propose a novel approach to integrating domain knowledge into CO problems addressed by RL methods, through the constraining of action spaces. Focusing on partitioning transportation networks, we aim to identify partitions with minimal Normalized Cut. Traditional methods like METIS are inadequate for this task, and current RL-based graph partitioning approaches often struggle

Table 1: Performance on Predefined-weight, Random-weight, and City Traffic Graphs by Normalized cut. Lower values indicate better performance.

Method	4 Partition					
	Predefined-weight		Random-weight		City Traffic	
	50	100	50	100	50	100
Metis	.069	.036	.065	.033	.245	.162
Spec. Clust.	.065	.036	.079	.041	.384	.218
Bruteforce	.070	.036	.070	.036	.361	.237
Random	.076	.040	.080	.041	.209	.095
NeuroCut	<u>.059</u>	<u>.032</u>	<u>.064</u>	<u>.033</u>	<u>.192</u>	<u>.078</u>
ClusterNet	.078	.043	.093	.043	.507	.261
WRT	.042	.021	.057	.029	.174	.060

Method	6 Partition					
	Predefined-weight		Random-weight		City Traffic	
	50	100	50	100	50	100
Metis	.097	.053	.094	<u>.049</u>	.383	.304
Spec. Clust.	.099	.053	.101	.053	.652	.843
Bruteforce	.106	.054	.107	.054	.615	.457
Random	.144	.074	.142	.072	.512	.341
NeuroCut	<u>.086</u>	<u>.046</u>	<u>.093</u>	<u>.049</u>	<u>.348</u>	<u>.226</u>
ClusterNet	.106	.070	.120	.083	.837	.747
WRT	.062	.032	.081	.041	.317	.182

when the initial partition produced by METIS is suboptimal. Furthermore, these methods fail to leverage domain knowledge to enhance their performance. We utilize domain knowledge indicating that ring and wedge partitions are effective for graph partitioning in transportation networks, and we provide proofs supporting this assertion. By implementing Ring and Wedge Transformations and transforming the action spaces into partition radii and angles, our approach effectively learns and optimizes the partitioning process. The two-stage training methodology ensures both stability and scalability, allowing WRT to efficiently manage graphs of varying sizes. Our experimental results demonstrate the superiority of our method compared to baseline algorithms, showcasing its potential for real-world applications. The findings illustrate the effectiveness of integrating domain knowledge and constrained action spaces. Future work will focus on addressing additional CO problems utilizing constrained action spaces by further harnessing domain knowledge.

References

- [1] Family of graph and hypergraph partitioning software, 2023.
- [2] Parmetis - parallel graph partitioning and fill-reducing matrix ordering, 2023.
- [3] Scotch: Software package and libraries for sequential and parallel graph partitioning, 2023.

Table 2: Transfer performance by Normalized Cut, only transferable methods are included. Trained on 100 nodes and tested on 50 or 200 nodes.

Method	4 Partition					
	Predefined-weight		Random-weight		City Traffic	
	50	200	50	200	50	200
METIS	<u>.069</u>	.019	<u>.065</u>	<u>.016</u>	.245	<u>.048</u>
Bruteforce	.070	<u>.018</u>	.070	.018	.361	.175
Random	.076	.021	.080	.021	<u>.209</u>	.512
WRT	.052	.013	.061	.016	.158	.023

Method	6 Partition					
	Predefined-weight		Random-weight		City Traffic	
	50	200	50	200	50	200
METIS	<u>.097</u>	<u>.027</u>	<u>.094</u>	<u>.024</u>	<u>.383</u>	<u>.086</u>
Bruteforce	.106	.028	.107	.028	.615	.311
Random	.144	.037	.142	.037	.512	.212
WRT	.066	.017	.087	.022	.323	.085

Table 3: Ringness and Wedgeness Evaluation, higher is better.

	METIS	Spec.Clust.	NeuroCUT	ClusterNet	WRT
Ringness	0.871	0.776	0.840	0.854	0.929
Wedgeness	0.587	0.810	0.621	0.820	0.876

- [4] F. M. Bianchi, D. Grattarola, and C. Alippi. Spectral clustering with graph neural networks for graph pooling. In *Proceedings of the 37th International Conference on Machine Learning*, volume 119 of *Proceedings of Machine Learning Research*, pages 874–883. PMLR, 2020.
- [5] S. Brody, U. Alon, and E. Yahav. How attentive are graph attention networks? In *The Tenth International Conference on Learning Representations, ICLR 2022*. OpenReview.net, 2022.
- [6] A. Buluç, H. Meyerhenke, I. Safro, P. Sanders, and C. Schulz. *Recent Advances in Graph Partitioning*, volume 9220. 11 2016.
- [7] F. R. K. Chung. *Spectral Graph Theory*, volume 92. CBMS Regional Conference Series in Mathematics, 1997.
- [8] R. Diekmann, R. Preis, F. Schlimbach, and C. Walshaw. *Parallel Computing*, 26(12):1555–1581, 2000.
- [9] W. E. Donath and A. J. Hoffman. Lower bounds for the partitioning of graphs. *IBM Journal of Research and Development*, 17(5):420–425, 1973.
- [10] H. Dong, H. Dong, Z. Ding, S. Zhang, and T. Chang. *Deep Reinforcement Learning*. Springer, 2020.

Table 4: Inference Time Comparison of different Methods

Size	METIS	Spectral	NeuroCUT	ClusterNet	WRT
50	0.073	0.011	0.845	0.140	0.050
100	0.062	0.034	1.596	0.145	0.073
200	0.077	0.507	2.512	0.140	0.261

- [11] C. Ferreira, A. Martin, C. Souza, R. Weismantel, and L. Wolsey. The node capacitated graph partitioning problem: A computational study. *Mathematical Programming*, 81:229–256, 01 1998.
- [12] A. Gatti, Z. Hu, T. Smidt, E. G. Ng, and P. Ghysels. *Deep Learning and Spectral Embedding for Graph Partitioning*, pages 25–36. 2022.
- [13] A. Gatti, Z. Hu, T. Smidt, E. G. Ng, and P. Ghysels. Graph partitioning and sparse matrix ordering using reinforcement learning and graph neural networks. *Journal of Machine Learning Research*, 23(303):1–28, 2022.
- [14] A. George and J. W. Liu. *Computer Solution of Large Sparse Positive Definite*. Prentice Hall Professional Technical Reference, 1981.
- [15] N. Grinsztajn. *Reinforcement learning for combinatorial optimization: leveraging uncertainty, structure and priors*. PhD thesis, Université de Lille, 2023.
- [16] W. Hager, D. Phan, and H. Zhang. An exact algorithm for graph partitioning. *Mathematical Programming*, 137, 12 2009.
- [17] L. Hyafil and R. L. Rivest. Graph partitioning and constructing optimal decision trees are polynomial complete problems. Technical Report Rapport de Recherche no. 33, IRIA – Laboratoire de Recherche en Informatique et Automatique, October 1973.
- [18] N. Karalias and A. Loukas. Erdos goes neural: an unsupervised learning framework for combinatorial optimization on graphs. In *Advances in Neural Information Processing Systems 33: Annual Conference on Neural Information Processing Systems 2020, NeurIPS 2020*, 2020.
- [19] G. Karypis, R. Aggarwal, V. Kumar, and S. Shekhar. Multilevel hypergraph partitioning: Application in VLSI domain. In *Proceedings of the 34th Conference on Design Automation, Anaheim, California, USA, Anaheim Convention Center, June 9-13, 1997*, pages 526–529. ACM Press, 1997.
- [20] G. Karypis, R. Aggarwal, V. Kumar, and S. Shekhar. Multilevel hypergraph partitioning: applications in VLSI domain. *IEEE Trans. Very Large Scale Integr. Syst.*, 7(1):69–79, 1999.
- [21] G. Karypis and V. Kumar. Parallel multilevel k-way partitioning scheme for irregular graphs. In *Supercomputing '96: Proceedings of the 1996 ACM/IEEE Conference on Supercomputing*, 1996.
- [22] G. Karypis and V. Kumar. A fast and high quality multilevel scheme for partitioning irregular graphs. *Siam Journal on Scientific Computing*, 20, 01 1999.
- [23] B. W. Kernighan and S. Lin. An efficient heuristic procedure for partitioning graphs. *The Bell System Technical Journal*, 49(2):291–307, 1970.
- [24] T. N. Kipf and M. Welling. Semi-supervised classification with graph convolutional networks. In *5th International Conference on Learning Representations, ICLR 2017*. OpenReview.net, 2017.
- [25] J. R. Lee, S. O. Gharan, and L. Trevisan. Multiway spectral partitioning and higher-order cheeger inequalities. *J. ACM*, 61(6), dec 2014.
- [26] H. Lemos, M. O. R. Prates, P. H. C. Avelar, and L. C. Lamb. Graph colouring meets deep learning: Effective graph neural network models for combinatorial problems. In *31st IEEE International Conference on Tools with Artificial Intelligence, ICTAI 2019*, pages 879–885. IEEE, 2019.
- [27] N. Mazyavkina, S. Sviridov, S. Ivanov, and E. Burnaev. Reinforcement learning for combinatorial optimization: A survey. *Computers & Operations Research*, 134:105400, 2021.
- [28] H. Meyerhenke, B. Monien, and T. Sauerwald. A new diffusion-based multilevel algorithm for computing graph partitions. *Journal of Parallel and Distributed Computing*, 69(9):750–761, 2009.
- [29] A. Y. Ng, M. I. Jordan, and Y. Weiss. On spectral clustering: Analysis and an algorithm. In T. G. Dietterich, S. Becker, and Z. Ghahramani, editors, *Advances in Neural Information Processing Systems 14 [Neural Information Processing Systems: Natural and Synthetic, NIPS 2001]*, pages 849–856. MIT Press, 2001.
- [30] F. Pellegrini. A parallelisable multi-level banded diffusion scheme for computing balanced partitions with smooth boundaries. 08 2007.
- [31] M. O. R. Prates, P. H. C. Avelar, H. Lemos, L. C. Lamb, and M. Y. Vardi. Learning to solve np-complete problems: A graph neural network for decision TSP. In *The Thirty-Third AAAI Conference on Artificial Intelligence, AAAI 2019*, pages 4731–4738. AAAI Press, 2019.

- [32] L. Rampásek, M. Galkin, V. P. Dwivedi, A. T. Luu, G. Wolf, and D. Beaini. Recipe for a general, powerful, scalable graph transformer. In *Advances in Neural Information Processing Systems 35: Annual Conference on Neural Information Processing Systems 2022, NeurIPS 2022*, 2022.
- [33] P. Sanders and C. Schulz. Engineering multi-level graph partitioning algorithms. In *Algorithms–ESA 2011: 19th Annual European Symposium, Saarbrücken, Germany, September 5-9, 2011. Proceedings 19*, pages 469–480. Springer, 2011.
- [34] J. Schulman, F. Wolski, P. Dhariwal, A. Radford, and O. Klimov. Proximal policy optimization algorithms. *arXiv preprint arXiv:1707.06347*, 2017.
- [35] R. Shah, K. Jain, S. Manchanda, S. Medya, and S. Ranu. Neurocut: A neural approach for robust graph partitioning. In *Proceedings of the 30th ACM SIGKDD Conference on Knowledge Discovery and Data Mining*, pages 2584–2595, 2024.
- [36] A. Tsitsulin, J. Palowitch, B. Perozzi, and E. Müller. Graph clustering with graph neural networks. *J. Mach. Learn. Res.*, 24:127:1–127:21, 2023.
- [37] A. Vaswani, N. Shazeer, N. Parmar, J. Uszkoreit, L. Jones, A. N. Gomez, Ł. Kaiser, and I. Polosukhin. Attention is all you need. *Advances in neural information processing systems*, 30, 2017.
- [38] P. Velickovic, G. Cucurull, A. Casanova, A. Romero, P. Liò, and Y. Bengio. Graph attention networks. In *6th International Conference on Learning Representations, ICLR 2018*. OpenReview.net, 2018.
- [39] Q. Wang and C. Tang. Deep reinforcement learning for transportation network combinatorial optimization: A survey. *Knowledge-Based Systems*, 233:107526, 2021.
- [40] B. Wilder, E. Ewing, B. Dilkina, and M. Tambe. End to end learning and optimization on graphs. *Advances in Neural Information Processing Systems*, 32, 2019.

A Statistics and Hyper Parameters

Table 5: Statistics of datasets and hyper parameters of model.

Type	Parameter	Values	Description
Synthetic	Nodes	{50, 100}	Nodes on each circle
	Circles	same as Nodes	Number of concentric rings
	Low Weight	{2, 4, 6}	Intra-partition edge weights
	High Weight	{10, 15, 20}	Inter-partition edge weights
	Random Weight	Uniform(1, 10)	Edge weights for random
Real	Nodes	{50, 100}	Nodes on each graph
	Edge Weight	[1, 372732]	Edge weights
Hyper Parameters	Partitions	{4,6}	Number of partitions
	Hidden Size	64	Hidden size of Transformer
	Layer Number	3	Transformer layer number
	Learning Rate	1e-3	Learning rate
	Batch Size	256	Batch size
	Discount Factor	0.9	Discount factor in RL
	Training Step	400,000	Steps for training
	Test Number	100	Test graph number
	Sample Number	10	Sampled partition number

B Ablation Studies

We propose ablation studies of WRT and its variants. They are: **WRT** the standard Wedge-Ring Partition with two-stage training. **WRT_{e2e}** directly learns Wedge-Ring Partition without two-stage training. **WRT_{sr}** uses the same reward function during two training stages. **WRT_o** does not performing post refinement after ring-wedge partition is generated. **WRT_{nfw}** does not freezing the wedge action network during the second training stage. Results of variants are in Appendix.

We give ablation studies in the following to show the effectiveness of proposed methods. The performance of ablation models are shown in Table 6 and 7.

B.1 Two-stage Training and Testing

In Section 5.5, we propose multi-stage training and testing strategies. In training, we propose to train the wedge partition model firstly, and randomly select ring partitions. The radius are uniformly selected from 0 to 80% of maximum radius. After wedge partition model is trained, we re-initialize the critic projection header of wedge model, and fix the other parts of wedge model to train the ring model part. We show the performance without two stage training as **WRT_{e2e}**. From Table 6 and Table 7, we can find that without two stage training, the model is not able to converge, because a bad policy of either ring or wedge will af-

Table 6: Performance comparison on Predefined-weight, Random-weight, and City Traffic Graphs (Normalized cut). Lower values indicate better performance.

Method	Predefined-weight				Random-weight				City Traffic			
	4 Part.		6 Part.		4 Part.		6 Part.		4 Part.		6 Part.	
	50	100	50	100	50	100	50	100	50	100	50	100
Metis	.069	.036	.097	.053	.065	.049	.094	.049	.245	.162	.383	.304
Spec. Clust.	.065	.036	.099	.053	.079	.053	.101	.053	.384	.218	.652	.843
Bruteforce	.070	.036	.106	.054	.070	.054	.107	.054	.361	.237	.615	.457
Random	.076	.040	.144	.074	.080	.072	.142	.072	.209	.095	.512	.341
NeuroCut	.059	.032	.086	.046	.064	.033	.093	.049	.192	.078	.348	.226
ClusterNet	.078	.043	.106	.070	.093	.043	.120	.083	.507	.261	.837	.747
WRT _{sr}	.063	.276	.065	.032	.159	.044	.091	.046	.646	.473	.792	.612
WRT _{e2e}	.105	.053	.123	.063	.112	.055	.131	.069	.683	.478	.783	.678
WRT _o	.042	.021	.062	.032	.057	.029	.081	.041	.209	.071	.419	.271
WRT _{nfw}	.046	.023	.065	.033	.057	.029	.082	.041	.175	.060	.328	.187
WRT	.042	.021	.062	.032	.057	.029	.081	.041	.174	.060	.317	.182

Table 7: Transfer performance measured by Normalized Cut. Methods that do not support transfer or unable to perform results are excluded. Models are trained on 100 nodes and tested on 50 or 200 nodes.

Partition	Predefined-weight				Random-weight				City Traffic			
	4 Part.		6 Part.		4 Part.		6 Part.		4 Part.		6 Part.	
	50	200	50	200	50	200	50	200	50	200	50	200
Nodes	50	200	50	200	50	200	50	200	50	200	50	200
METIS	.069	.019	.097	.027	.065	.016	.094	.024	.245	.048	.383	.086
Bruteforce	.070	.018	.106	.028	.070	.018	.107	.028	.361	.175	.615	.311
Random	.076	.021	.144	.037	.080	.021	.142	.037	.209	.512	.512	.212
WRT _{sr}	.219	.201	.068	.018	.085	.023	.092	.024	.664	.305	.831	.224
WRT _{e2e}	.103	.027	.107	.027	.107	.028	.123	.033	.645	.327	.863	.442
WRT _o	.052	.013	.066	.016	.061	.016	.087	.022	.182	.031	.472	.014
WRT _{nfw}	.053	.013	.066	.017	.061	.016	.087	.104	.150	.023	.327	.090
WRT	.052	.013	.066	.017	.061	.016	.087	.022	.158	.023	.323	.085

Table 8: Performance comparison on City Traffic Graphs (Normalized cut). Lower values indicate better performance.

Method	City Traffic			
	4 Part.		6 Part.	
	50	100	50	100
GPS	0.696	0.521	0.821	0.711
Transformer	0.186	0.122	0.360	0.225
WRT w/o PAMHA	0.169	0.075	0.374	0.193
WRT	0.174	0.060	0.317	0.182

fect the learning process of each other, and make the model hard to converge.

B.2 Different Baseline Function in Two-stage

As mentioned in Section 5.5, in training wedge partition, we change the reward function from global Normalized Cut to the Normalized Cut that only considering wedge partitions. This avoids the impact of poor ring partition selection, as ring partition is performed by a random policy, and may give poor partitions. For example, if the random policy selects a very small radius, the normalized cut of circle partitions will be very big, which makes the reward received from different wedge partition identical. We show the performance when the reward function keeps same, i.e. always considering the normalized cut of ring partition in two stage training, as WRT_{sr}. In Table 6 and 7, we can find that their performance is worse than WRT, because their wedge partitioning policies are not strong enough. As reward function will change in two-stage training, we will re-initialize the

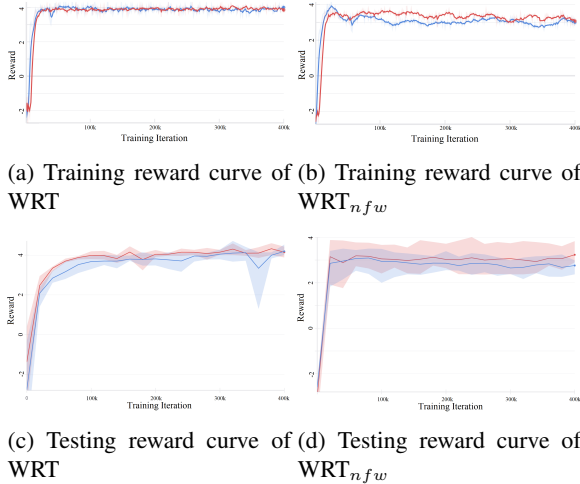


Figure 7: Reward curves during training and testing of Predefined-weight Graph. Red is with 50 node number and blue is with 100 node number. We individually perform 4 tests for each checkpoint, using the curve to represent the average test results, while the shaded area indicates the maximum and minimum values observed during the tests.

critic net of wedge model in the second stage, as mentioned before.

B.3 Fix Wedge Partition Policy

In the second training stage, we fix the wedge model to avoid changing the policy. WRT_{nfw} shows the performance when wedge partition policy is not fixed. We can find that the performance decreases if wedge partition policy is not fixed, and leads to bad policy in several test cases. This is because if we allow the action net change, it may forget learned policy before a valid policy has learned by ring partition, and leads to worse performance and instability during the training. The reward curve during training and testing, which is shown in Figure 7, also supports the conclusion. It has been observed that not fixing the action net results in lower and more unstable rewards for the model during training. Moreover, the performance during testing tends to become more variable and does not show further improvements as training progresses.

B.4 Post Refinement

We perform post refinement after performing the ring and wedge partition, which splits existing partition result by the connectivity of nodes, then reconstruct new partitions by combining the partition which has biggest Normalized Cut with its adjacent partitions. As ring and wedge partitions on synthetic graphs are always connected, this

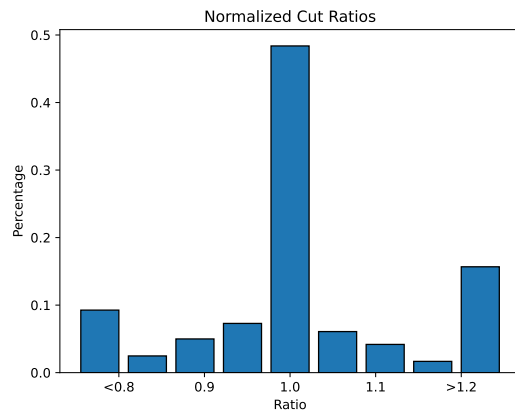
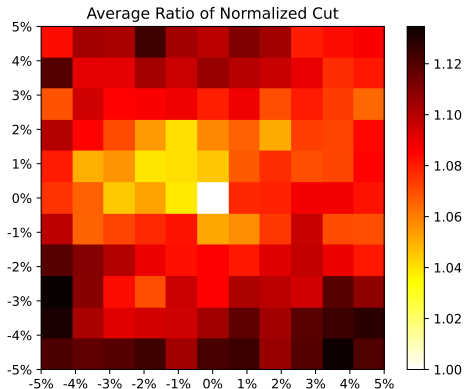


Figure 8: Heatmap and histogram of Normalized Cut when applying offsets to the center. Values are normalized by Normalized Cut of unoffset center. Lower value is better.

post refinement will not change the performance of WRT on synthetic dataset. However, in real dataset, sometimes the graph shape is not compatible to ring and wedge partition, and the results may not good enough. With post refinement, we can further decrease the Normalized Cut on such situation. In Table 6, we show the performance improvements with post refinement on real dataset, the normalized cut is decreased 22.4% on average.

B.5 Graph Center Selection

We conducted experiments on the test set of City Traffic graphs with 50 nodes, which contains 100 graphs. Based on the maximum aspect ratio of the graphs, we offset the centroid by a distance of up to 5% and recalculated the results of Normalized Cut. For better comparison, we normalized the results using the Normalized Cut from the unoffset scenario. A normalized value closer to zero indicates better performance, with a value of 1 signifying that the results are the same as in the unoffset case.

Figure 8 (left) illustrates the results for various offsets from the centroid. We observe that any offset from the centroid results in a worse performance, and with greater offsets correlating to a more significant decline.

In Figure 8 (right), we present the histogram of results across all the aforementioned offsets and graphs. We find that in nearly half of the cases where offsets were applied, the resulting errors remained within 5%. Furthermore, applying offsets tends to lead to worse outcomes more frequently. Thus, in this paper, we opted to use the centroid as the center of the graph. Figure 8 (right) also shows that in approximately 15% of cases, offsetting the centroid yielded improvements of over 10%. In the future, we can propose a more effective strategy for centroid selection to enhance the algorithm’s performance.

B.6 Effectiveness of Graph Transformation, WRT and PAMHA

We demonstrate the effectiveness of our proposed Graph Transformation methods, WRT and PAMHA, as presented in Table 8. The methods evaluated are as follows:

- GPS [32]: It integrates GNNs and Transformers to effectively capture both local and global information. It serves as the benchmark for evaluating the performance of GNNs and Transformers in addressing the Normalized Cut problem using Ring and Wedge Partition techniques.
- Transformer: We implement Ring and Wedge Transformations on the graph, utilizing node coordinates as positional embeddings and edge weights as attention masks, followed by the application of a standard Transformer model.
- WRT w/o PAMHA: This configuration maintains the same architecture as WRT but substitutes PAMHA with conventional Multi-Head Attention.

From the results, we observe that GPS struggles to produce meaningful results in City Traffic. In contrast, the Transformer model demonstrates significantly improved outcomes when compared to GPS. This finding reinforces the notion that constraining the action space of RL agents based on domain knowledge is essential for enhancing performance. Next, we integrated the WRT structure, which facilitates data pre-calculation, and observed an increase in performance. This indicates that the pre-calculation module is beneficial in addressing the problem. Finally, by incorporating PAMHA into the Transformer framework, we achieved the full WRT architecture, which exhibited superior performance relative to other variants.

Table 9: Performance comparison on City Traffic Graphs (Normalized cut). Lower values indicate better performance.

Method	City Traffic			
	4 Part.		6 Part.	
	50	100	50	100
DMon	0.998	1.000	1.000	1.000
MinCutPool	0.549	0.365	0.864	0.634
Ortho	0.924	0.892	0.997	0.982
WRT	0.174	0.060	0.317	0.182

Table 10: Comparison of Hidden State and Learning Rate for Different Methods.

	Hidden State	Learning Rate
Search Range	16, 32, 64, 128, 256	1e-4, 3e-4, 1e-3, 3e-3, 1e-2
Dmon	128	1e-4
MinCutPool	32	1e-3
Ortho	256	1e-2

B.7 Performance of Other Methods

We incorporate additional comparative methods Analyzed on City Traffic Graph, which include:

- DMon [36]: A neural attributed graph clustering method designed to effectively handle complex graph structures.
- MinCutPool [4]: This method focuses on optimizing the normalized cut criterion while incorporating an orthogonality regularizer to mitigate unbalanced clustering outcomes.
- Ortho [36]: This refers to the orthogonality regularizer that is utilized in both DMon and MinCutPool, ensuring greater balance in the clustering process.

All models were trained using the same settings as WRT. We conducted a grid search on the hyperparameters of the three aforementioned methods and selected the optimal combination of hyperparameters to train on other datasets. The search range and the selected hyperparameters are detailed in Table 10. The results are summarized in Table 9. From the findings, it is evident that Dmon fails to effectively learn the partition strategy, resulting in most outcomes being invalid (with Normalized Cut values of 1). Ortho performs slightly better but still tends to yield unbalanced results. In contrast, MinCutPool demonstrates a significant improvement over the previous methods; however, it still exhibits a considerable range compared to our proposed WRT.

C Detail of the Model Pipeline

We detail the model transformation formulas below. Since the processes for ring and wedge partitioning are similar, we focus on the wedge partitioning pipeline and note the differences later.

Let G be the input graph and P the current partition. We apply Wedge Transformation to G to obtain a linear graph G' . Define n_i as the i -th node on this line, with n candidate actions. Action a_i corresponds to selecting the radius of the ring partition between n_i and n_{i+1} . The input embedding is constructed as follows:

$$\mathbf{X}_i = \text{Linear}_{CW}(\text{Cut}_i \oplus \text{PS}_i) + \text{Pos}_{i/|N|} \rightarrow \mathbb{R}^d,$$

where Linear_{CW} is a linear transformation, Cut_i is the Cut Weight between n_i and n_{i+1} , PS_i is the Partition Selection for n_i , and $\text{Pos}_{i/|N|}$ is the positional embedding scaled based on the total number of nodes.

In WRT, we derive the attention masks M^P and M^V as follows:

$$M_{i,j}^P = \begin{cases} 0 & \text{if } i \text{ and } j \text{ are in the same partition} \\ -\infty & \text{otherwise} \end{cases}, \quad (8)$$

$$M_{i,j}^V = \text{Linear}_V(V_{i,j}).$$

When nodes i and j are in different partitions, the attention weight is set to $-\infty$ to prevent their influence on each other. Denote $H_i^0 = X_i$; the t -th hidden states H_i^t are computed as follows:

$$\mathbf{Q}^t, \mathbf{K}^t, \mathbf{V}^t = \text{Linear}_{\text{Att}}(\mathbf{H}^t), \quad (9)$$

$$\mathbf{O}^t = \text{Softmax}(\mathbf{Q}\mathbf{K}^t + \mathbf{M}^V + \mathbf{M}^P). \quad (10)$$

The output for each node at the t -th layer is:

$$Y_i^t = \text{LayerNorm} \left(\sum_{k=1}^N O_{i,k}^t V_k / \sqrt{d} + H_i^t \right), \quad (11)$$

$$H_i^{t+1} = \text{LayerNorm}(Y_i^t + \text{FFN}(Y_i^t)). \quad (12)$$

The Transformer has T layers, with $\mathbf{E} = \mathbf{H}^T$ as the output embeddings.

In the PPO module, we calculate action probabilities and predicted values using \mathbf{E} :

$$\text{Logit}_i = \text{Linear}_A(E_i) \rightarrow \mathbb{R}, \quad (13)$$

$$\mathbf{Prob} = \text{Softmax}(\text{Logit}), \quad (14)$$

$$\text{PredictedValue} = \text{Linear}_{PV}(\text{Attention}(\mathbf{E})) \rightarrow \mathbb{R}. \quad (15)$$

We sample actions from the probability distribution and train the model using rewards and predicted values.

For ring partitioning, two key differences arise. First, we employ Ring Transformation on the graph. Second, the

positional embedding is 2-dimensional, reflecting the adjacency of the first and last nodes. Specifically, for a circular node with coordinates (x, y) , we use:

$$PE = \text{Linear}_{2D}(x \oplus y) \rightarrow \mathbb{R}^d$$

to generate the positional embedding.

D Definition of Ringness and Wedgeness

We propose the Ringness and Wedgeness to evaluate whether a partition is close to the ring shape or wedge shape. We expect a typical Ring and Wedge partition will have the highest Ringness and Wedgeness.

For partition $p_i \in P$, we define the partition range $pr_i = \{\min(\mathbf{r}_i), \max(\mathbf{r}_i)\}$, partition angle $pa_i = \{\min(\mathbf{a}_i), \max(\mathbf{a}_i)\}$, where \mathbf{r}_i and \mathbf{a}_i are polar coordinates of nodes that belongs to p_i .

Then we define Ringness for a partition $R_P(r) = |\{r \in pr_i\}|$, which means that how many partitions cover the radius r . For a pure ring partition, as different partitions will never overlap within their radius, $R_P(r)$ will be always 1; and for a Ring and Wedge partition, $R_P(r)$ is always 1, except the out-most wedge part, is the wedge partition number k_w .

For Wedgeness, we define $W_P(r) = \sum_{r \in pr_i} |pa_i|$, where $|pa_i|$ is the angle range of pa_i . For radius r , we only consider the partition that covers the selected range, and we sum up the angles covered by these partitions. The angle should equal or greater than 2π , as the graph is fully partitioned by P . If a partition is a pure wedge partition, for any r , the Wedgeness should be exactly 2π , because partition will never cover each other in any place. For Ring and Wedge Partition, if r is in Wedge Partition part, the conclusion remains same as above; for Ring Partition part, only one partition is selected, and the Wedgeness is also 2π .

To represent Ringness and Wedgeness more clearly, we calculate the quantification metrics for them based on the following formula:

$$\mathbf{W}_P = \frac{Z(P) - \min_{0 \leq k \leq \max(\mathbf{r})} \left(\int_{i=0}^k W_P(i) + \int_{i=k}^{\max(\mathbf{r})} (\max(W) - W_P) \right)}{Z(P)} \quad (16)$$

$$\mathbf{R}_P = \frac{2\pi}{\max_r R_P(r)} \quad (17)$$

$$f(x) = \begin{cases} 1 & \text{if } 0 \leq x \leq k \\ \max(W) & \text{if } k < x \leq \max(\mathbf{r}) \end{cases} \quad (18)$$

Here $Z(P) = 0.5 \max(\mathbf{r}) \cdot \max(W)$ is the normalization factor. We use a piecewise function f to approximate W_P , and provide \mathbf{W}_P based on the difference between W_P and f . For \mathbf{R}_P , we select the maximum of R_p . Both \mathbf{W}_P and \mathbf{R}_P is scaled to $[0, 1]$, and the higher means the better.

E Proofs of Cheeger Bounds

E.1 Proof of Proposition 1

In this section we will provide all the details of the proof of Proposition 1. First we recall some background definitions and results.

Let $G = (V, E)$ be an undirected graph with $|V| = n$. Let D be the diagonal matrix with the node degrees on the diagonal and let $L = D^{-\frac{1}{2}}(D - A)D^{-\frac{1}{2}}$ be the normalized Laplacian of G ¹, where A is the adjacency matrix of G . The matrix L is positive semi-definite with eigenvalues

$$0 = \lambda_1 \leq \lambda_2 \leq \dots \leq \lambda_n. \quad (19)$$

For a subset $S \subseteq V$ define

$$\phi_G(S) = \frac{Cut(S, S^c)}{Volume(S)} \quad (20)$$

and, for $1 \leq k \leq n$, we define the *Cheeger constants*

$$\rho_G(k) = \min_{\substack{S_1, \dots, S_k \\ \text{partition of } V}} \max_{1 \leq i \leq k} \phi_G(S_i). \quad (21)$$

It is known that, for $k = 2$, the following inequalities hold [7]

$$\frac{\lambda_2}{2} \leq \rho_G(2) \leq \sqrt{2\lambda_2}. \quad (22)$$

Analogous inequalities were proved in [25] for every $1 \leq k \leq n$

$$\frac{\lambda_k}{2} \leq \rho_G(k) \leq \mathcal{O}(k^2)\sqrt{\lambda_k}. \quad (23)$$

If G is planar, then the right-side inequality can be improved and reads

$$\rho_G(k) \leq \mathcal{O}(\sqrt{\lambda_{2k}}). \quad (24)$$

Now let $G_{N,r} = (V, E)$ be an undirected spider web graph with r rings and N points for each ring. This is exactly the cartesian product of a circle graph and a path graph with N and r vertices respectively. Note that the ‘‘center’’ is not included in this type of graphs. Define the following custom Cheeger constants:

$$\varphi_{N,r}(k) = \min_{\substack{S_1, \dots, S_k \\ \text{wedge partition of } V}} \max_{1 \leq i \leq k} \phi_{G_{N,r}}(S_i) \quad (25)$$

$$\psi_{N,r}(k) = \min_{\substack{S_1, \dots, S_k \\ \text{ring partition of } V}} \max_{1 \leq i \leq k} \phi_{G_{N,r}}(S_i). \quad (26)$$

For an illustration of wedge and ring partitions see Figure 9. From now on we will assume $G = G_{N,r}$ to be a spider web graph with r rings and N points for each ring. We can compute bounds on $\varphi_{N,r}(k)$ and $\psi_{N,r}(k)$.

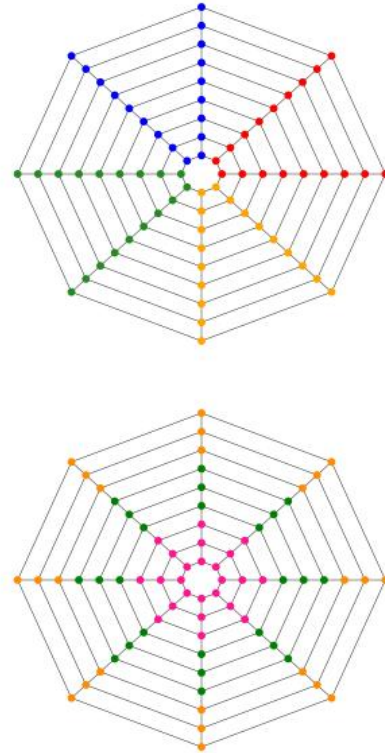


Figure 9: Examples of $k = 4$ wedge (left) and $k = 3$ ring (right) partitions.

¹For the sake of simplicity, often it will be called just Laplacian.

Lemma 1. *Given a spider-web graph $G_{N,r}$ the wedge and ring Cheeger constants can be bounded as follows*

$$\varphi_{N,r}(k) \leq \frac{r}{\lfloor \frac{N}{k} \rfloor (2r-1)}, \quad \psi_{N,r}(k) \leq \frac{1}{2\lfloor \frac{r}{k} \rfloor}. \quad (27)$$

Proof. The strategy will be to choose suited partitions for which it is possible to compute explicitly the cuts and the volumes. We start from the wedge Cheeger constant $\varphi_{N,r}(k)$. Given a wedge partition S_1, \dots, S_k each subset S_i has cut exactly $2r$. Moreover, we assume that the S_i 's are maximally symmetric, meaning that the S_i 's all have $\lfloor \frac{N}{k} \rfloor$ or $\lfloor \frac{N}{k} \rfloor + 1$ nodes in each ring. These observation read

$$\begin{aligned} \varphi_{N,r}(k) &\leq \max_{1 \leq i \leq k} \frac{2r}{\text{Volume}(S_i)} \\ &= \frac{2r}{\min_{1 \leq i \leq k} \text{Volume}(S_i)}. \end{aligned} \quad (28)$$

The wedge subset with minimum volume is given by one that has $\lfloor \frac{N}{k} \rfloor$ nodes in each ring, hence

$$\begin{aligned} \varphi_{N,r}(k) &\leq \frac{2r}{\underbrace{4}_{\substack{\text{degree of} \\ \text{inner ring} \\ \text{nodes}}} \underbrace{(r-2)}_{\substack{\text{number of} \\ \text{inner rings}}} \underbrace{\lfloor \frac{N}{k} \rfloor}_{\substack{\text{number of} \\ \text{points in} \\ \text{each ring}}} + \underbrace{3}_{\substack{\text{degree of} \\ \text{outer ring} \\ \text{nodes}}} \underbrace{2}_{\substack{\text{number of} \\ \text{outer rings}}} \underbrace{\lfloor \frac{N}{k} \rfloor}_{\substack{\text{number of} \\ \text{points in} \\ \text{each ring}}}} \\ &= \frac{r}{\lfloor \frac{N}{k} \rfloor (2r-1)}. \end{aligned} \quad (29)$$

For the ring Cheeger constant the setting is more complicated since different subsets might have different cut, in contrast with the case of wedge partitions. Given a ring partition S_1, \dots, S_k which is maximally symmetric, i.e., all the S_i 's have $\lfloor \frac{r}{k} \rfloor$ or $\lfloor \frac{r}{k} \rfloor + 1$ nodes in each ring, we order the S_i 's from the center to the outermost ring. Note that S_1 has some nodes with degree 3 while S_2 has all nodes with degree 4 for $k > 2$. For $k \geq 2$, we consider two cases:

- k divides r . In this case we only need to compare S_1 and S_2 . It holds that

$$\phi_G(S_1) = \frac{N}{4N(\frac{r}{k}-1) + 3N} = \frac{1}{4\frac{r}{k}-1} \quad (30)$$

$$\phi_G(S_2) = \frac{2N}{4N\frac{r}{k}} = \frac{1}{2\frac{r}{k}}, \quad (31)$$

since S_1 and S_2 have cut N and $2N$ respectively. Thus, $\phi_G(S_2) \geq \phi_G(S_1)$ which implies $\psi_{N,r}(k) \leq \frac{1}{2\frac{r}{k}}$.

- k does not divide r . In this case, we assume S_1 has $\lfloor \frac{r}{k} \rfloor + 1$ nodes and S_2 has $\lfloor \frac{r}{k} \rfloor$ nodes. Then

$$\phi_G(S_1) = \frac{N}{4N\lfloor \frac{r}{k} \rfloor + 3N} = \frac{1}{4\lfloor \frac{r}{k} \rfloor + 3} \quad (32)$$

$$\phi_G(S_2) = \frac{2N}{4N\lfloor \frac{r}{k} \rfloor} = \frac{1}{2\lfloor \frac{r}{k} \rfloor}. \quad (33)$$

Thus, $\phi_G(S_2) \geq \phi_G(S_1)$ which implies $\psi_{N,r}(k) \leq \frac{1}{2\lfloor \frac{r}{k} \rfloor}$.

For $k = 2$, if k divides r , then $\phi_G(S_1) = \phi_G(S_2) = \frac{1}{4\frac{r}{k}-1} \leq \frac{1}{2\frac{r}{k}}$. If k does not divide r , then if S_1 has $\lfloor \frac{r}{k} \rfloor + 1$ nodes and S_2 has $\lfloor \frac{r}{k} \rfloor$ nodes, we have $\phi_G(S_1) = \frac{1}{4\lfloor \frac{r}{k} \rfloor + 3}$ and $\phi_G(S_2) = \frac{1}{4\lfloor \frac{r}{k} \rfloor - 1} \leq \frac{1}{2\lfloor \frac{r}{k} \rfloor}$. Putting together the above inequalities, we get that $\psi_{N,r}(k) \leq \frac{1}{2\lfloor \frac{r}{k} \rfloor}$. \square

In the next sections we will provide the proof details for the two bounds in Proposition 1. We start from the case of wedge partitions.

E.1.1 Wedge partitions

We will prove the bound on wedge Cheeger constants in terms of the eigenvalues of the circle graph with N vertices C_N . We will consider only the case of $k > 1$ since the first eigenvalue is always 0 and spider web graphs are connected. First we recall that the eigenvalues of C_N are

$$1 - \cos\left(\frac{2\pi k}{N}\right), \quad 0 \leq k \leq N-1, \quad (34)$$

see [7]. In particular, we have the following result.

Lemma 2. *Let C_N be the circle graph with N vertices. Then the k -th eigenvalues of the normalized Laplacian of C_N is given by*

$$\lambda_k^C = 1 - \cos\left(\frac{2\pi \lfloor \frac{k}{2} \rfloor}{N}\right), \quad 1 \leq k \leq N. \quad (35)$$

Proof. If we order the values of $\left\{1 - \cos\left(\frac{2\pi(k-1)}{N}\right)\right\}_{k=1}^N$ we notice that

$$\lambda_k^C = \begin{cases} f(\frac{k}{2}) & \text{if } k \in 2\mathbb{Z} \\ f(\frac{k-1}{2}) & \text{if } k \notin 2\mathbb{Z} \end{cases} \quad (36)$$

where $f(k) = 1 - \cos\left(\frac{2\pi k}{N}\right)$. Writing together the two pieces in (36) we get

$$\lambda_k^C = 1 - \cos\left(\frac{2\pi \lfloor \frac{k}{2} \rfloor}{N}\right), \quad 1 \leq k \leq N. \quad (37)$$

\square

Now we will prove some inequalities that together will build the final wedge Cheeger inequality.

Lemma 3. $\pi \lfloor \frac{k}{2} \rfloor \frac{1}{N} \leq \frac{\pi}{2}$, for $2 \leq k \leq N$.

Proof. Since $k \leq N$ we have the following inequality

$$\pi \lfloor \frac{k}{2} \rfloor \frac{1}{N} \leq \pi \lfloor \frac{N}{2} \rfloor \frac{1}{N} \begin{cases} = \frac{\pi}{2} & \text{if } k \in 2\mathbb{Z} \\ = \pi \frac{N-1}{2} \frac{1}{N} \leq \frac{\pi}{2} & \text{if } k \notin 2\mathbb{Z} \end{cases} \quad (38)$$

\square

Lemma 4. $2\lfloor \frac{k}{2} \rfloor \geq \frac{k}{2}$, for $2 \leq k \leq N$.

Proof. If k is even then $2\lfloor \frac{k}{2} \rfloor = 2\frac{k}{2} \geq \frac{k}{2}$. If k is odd, then $2\lfloor \frac{k}{2} \rfloor = 2\frac{k-1}{2} = k-1 \geq \frac{k}{2}$ for $2 \leq k \leq N$. \square

Lemma 5. $\sqrt{\lambda_k^C} \geq \frac{\sqrt{2}}{4} \frac{1}{\lfloor \frac{N}{k} \rfloor}$, for $2 \leq k \leq N$.

Proof. It holds that

$$\sqrt{\lambda_k^C} = \sqrt{1 - \cos\left(\frac{2\pi\lfloor \frac{k}{2} \rfloor}{N}\right)} \quad (39)$$

$$= \sqrt{2} \sin\left(\frac{\pi\lfloor \frac{k}{2} \rfloor}{N}\right) \quad (40)$$

$$\geq \sqrt{2} \frac{2}{\pi} \left(\frac{\pi\lfloor \frac{k}{2} \rfloor}{N}\right) \quad (41)$$

$$= 2\sqrt{2} \lfloor \frac{k}{2} \rfloor \frac{1}{N} \quad (42)$$

$$\geq \sqrt{2} \frac{k}{2} \frac{1}{N} \quad (43)$$

$$\geq \frac{\sqrt{2}}{2} \frac{1}{\lfloor \frac{N}{k} \rfloor + 1} \quad (44)$$

$$\geq \frac{\sqrt{2}}{2} \frac{1}{2\lfloor \frac{N}{k} \rfloor} \quad (45)$$

$$= \frac{\sqrt{2}}{4} \frac{1}{\lfloor \frac{N}{k} \rfloor} \quad (46)$$

where (39) follows from Lemma 2, (40) follows from the fact that $\cos(2x) = 1 - 2\sin^2(x)$, (41) follows from the fact that $\frac{\sin(x)}{x} > \frac{2}{\pi}$ for $x \in [-\frac{\pi}{2}, \frac{\pi}{2}]$ and from Lemma 3, (43) follows from Lemma 4. \square

Combining the results in Lemma 5 together with the ones in Lemma 1 we get the following result.

Proposition 2. For a spider web graph $G_{N,r}$ we have

$$\varphi_{N,r}(k) \leq \frac{2r}{2r-1} \sqrt{2\lambda_k^C}, \text{ for } 2 \leq k \leq N.$$

E.1.2 Ring partitions

Similarly as for wedge partitions, we will prove a bound on the ring Cheeger constants in terms of the eigenvalues of the path graph with r vertices P_r . Some of the computations are analogous to the ones in the previous section, so we will skip the details for these.

We recall that the eigenvalues of P_r are

$$\lambda_k^P = 1 - \cos\left(\frac{\pi(k-1)}{r-1}\right), \quad 1 \leq k \leq r, \quad (47)$$

see [7]. We have the following inequality for the ring Cheeger constant.

Lemma 6. $\sqrt{\lambda_k^P} \geq \frac{\sqrt{2}}{2} \frac{1}{2\lfloor \frac{r}{k} \rfloor}$, for $2 \leq k \leq r$.

Proof. It holds that

$$\sqrt{\lambda_k^P} = \sqrt{1 - \cos\left(\frac{\pi(k-1)}{2(r-1)}\right)} \quad (48)$$

$$= \sqrt{2} \sin\left(\frac{\pi(k-1)}{2(r-1)}\right) \quad (49)$$

$$\geq \sqrt{2} \frac{2}{\pi} \left(\frac{\pi(k-1)}{2(r-1)}\right) \quad (50)$$

$$\geq \frac{\sqrt{2}}{2} \frac{k}{r-1} \quad (51)$$

$$= \frac{\sqrt{2}}{2} \frac{1}{\frac{r}{k} - \frac{1}{k}} \quad (52)$$

$$\geq \frac{\sqrt{2}}{2} \frac{1}{\lfloor \frac{r}{k} \rfloor + 1 - \frac{1}{k}} \quad (53)$$

$$\geq \frac{\sqrt{2}}{2} \frac{1}{2\lfloor \frac{r}{k} \rfloor} \quad (54)$$

$$\geq \frac{\sqrt{2}}{2} \frac{1}{2\lfloor \frac{r}{k} \rfloor} \quad (55)$$

where the inequality (54) follows from the fact that

$$\lfloor \frac{r}{k} \rfloor + 1 - \frac{1}{k} \leq 2\lfloor \frac{r}{k} \rfloor. \quad (56)$$

\square

Combining the results in Lemma 5 together with the ones in Lemma 6 we get the following result.

Proposition 3. For a spider web graph $G_{N,r}$ we have

$$\psi_{N,r}(k) \leq \sqrt{2\lambda_k^P}, \text{ for } 2 \leq k \leq N.$$

F Pseudo Codes of Algorithms

In this section we give pseudo codes for algorithms, including Ring and Wedge Transformation, Volume and Cut calculation, WRT, PPO and full training pipeline.

We also provide the anonymized source code in the following link: <https://anonymous.4open.science/r/K24-00F8/>

Algorithm 1: Ring Transformation

Input: graph $G = (V, E, W, o)$
Output: Converted line graph G_l
 $r \leftarrow$ radius of $V - o$;
for each element i from 1 to $|r|$ **do**
 // rank of $r[i]$ in the sorted list of r
 $\text{Index}[i] \leftarrow \sum_{j=1}^n \mathbf{1}(r[j] \leq r[i])$;
for each element i from 1 to $|E|$ **do**
 $E_{new}[i] \leftarrow \{\text{Index}[E[i].x], \text{Index}[E[i].y]\}$;
for each element i from 1 to $|V|$ **do**
 $V_{new}[i] \leftarrow (\text{Index}[i], 0)$;
return $G_c = (V_{new}, E_{new}, W, (0, 0))$

Algorithm 2: Wedge Transformation

Input: graph $G = (V, E, W, o)$
Output: Converted circle graph G_c
 $a \leftarrow$ angles of $V - o$;
for each element i from 1 to $|a|$ **do**
 // rank of $a[i]$ in the sorted list of a
 $\text{Index}[i] \leftarrow \sum_{j=1}^n \mathbf{1}(a[j] \leq a[i])$;
for each element i from 1 to $|a|$ **do**
 $a_{new}[i] \leftarrow \frac{2\pi}{|a|} \text{Index}[i]$;
for each element i from 1 to $|E|$ **do**
 $E_{new}[i] \leftarrow \{a_{new}[E[i].x], a_{new}[E[i].y]\}$;
for each element i from 1 to $|a_{new}|$ **do**
 $V_{new}[i] \leftarrow (\sin(a_{new}[i]), \cos(a_{new}[i]))$;
return $G_c = (V_{new}, E_{new}, W, (0, 0))$

Algorithm 3: Volume and Cut for Line

Input: Line graph $G_l = (V, E, W, o)$
Output: Cut Cut and Volume $Volume$
 $a \leftarrow$ angles of $V - o$;
for e, w in E, W **do**
 if $e.x < e.y$ **then**
 $x, y \leftarrow e.x, e.y$
 else
 $x, y \leftarrow e.y, e.x$
 for i from x to y **do**
 $Cut[i] \leftarrow Cut[i] + w$;
 for i from 1 to x **do**
 for j from y to $|V|$ **do**
 $Volume[i, j] \leftarrow Volume[i, j] + w$;
return $Cut, Volume$

Algorithm 4: Volume and Cut for Circle

Input: Circle graph $G_c = (V, E, W, o)$
Output: Cut Cut and Volume $Volume$
 $a \leftarrow$ angles of $V - o$;
for e, w in E, W **do**
 $x, y \leftarrow e.x, e.y$ **if** $e.x > e.y$ **then**
 $y \leftarrow y + |V|$;
 for i from x to y **do**
 $Cut[i \% |V|] \leftarrow Cut[i \% |V|] + w$;
 for i from 1 to x **do**
 for j from y to $|V|$ **do**
 $Volume[i, j] \leftarrow Volume[i, j] + w$;
for i from 1 to $|V|$ **do**
 for j from 1 to $i - 1$ **do**
 // when $i > j$, means the direction that cross
 n-to-1 part
 $Volume[i, j] = Volume[j, i]$;
return $Cut, Volume$

Algorithm 5: WRT Transformer with Ring Partition

Input: Line graph $G_l = (V, E, W, o)$, current partition P
Output: Embeddings for each nodes emb
 $Cut, Volume \leftarrow Alg4(G_c)$;
// shape $[N, 1]$ to $[N, H]$;
 $x \leftarrow Linear(Cut)$;
// shape $[N, N, 1]$ to $[N, N, H]$ to $[N, N, 1]$;
 $VMask \leftarrow Linear(Volume)$;
 $PMask[i, j] \leftarrow 0$ if i and j are in same partition ;
 $PMask[i, j] \leftarrow -\infty$ if i and j are in different partition ;
// Pos is positional embedding, in circle partition, just same as normal NLP Transformer
 $H_0 = x + Pos$;
// L is layer number ;
for i from 1 to L **do**
 $Q, K, V \leftarrow Linear(H_{i-1})$;
 $A \leftarrow QK^T + VMask + PMask$;
 $H'_i \leftarrow Norm(AV) + H_{i-1}$;
 $H_i \leftarrow Norm(Linear((H'_i)) + H'_i)$;
return H_L

Algorithm 6: WRT Transformer with Wedge Partition

Input: Circle graph $G_l = (V, E, W, o)$, current partition P
Output: Embeddings for each nodes emb
 $Cut, Volume \leftarrow \text{Algorithm3}(G_c)$;
// shape $[N, 1]$ to $[N, H]$;
 $x \leftarrow \text{Linear}(Cut)$;
// shape $[N, N, 1]$ to $[N, N, H]$ to $[N, N, 1]$;
 $VMask \leftarrow \text{Linear}(Volume)$;
 $PMask[i, j] \leftarrow 0$ if i to j are in same partition ;
 $PMask[i, j] \leftarrow -\infty$ if i and j are in different partition ;
// Pos is positional embedding, x-y coords on the circle $H_0 = x + \text{Pos}$;
// L is layer number ;
for i from 1 to L **do**
 $Q, K, V \leftarrow \text{Linear}(H_{i-1})$;
 $A \leftarrow QK^T + VMask + PMask$;
 $H'_i \leftarrow \text{Norm}(AV) + H_{i-1}$;
 $H_i \leftarrow \text{Norm}(\text{Linear}(H'_i)) + H'_i$;
return H_L

Algorithm 7: PPO with Embeddings

Input: Embeddings for each nodes, i.e. actions, emb
Output: Action policy logits a , and critic for current state v
// $[N, H]$ to $[N, H]$ to $[N, 1]$;
 $a \leftarrow \text{Linear}(\text{Activate}(\text{Linear}(emb)))$;
// $[N, H]$ to $[1, H]$ to $[1, 1]$;
 $c \leftarrow \text{Linear}(\text{Activate}(\text{Attention}(emb)))$;
return a, c

G Dynamic Programming Algorithm for Ring Partition Phase

We show the pseudo-code of dynamic programming algorithm used in Ring Partition phase in Algorithm 9. This allows us performing ring partition only once. The time complexity of this algorithm is $O(n^2k)$. The DP matrix $dp[i, j]$ stores the minimum normalized cut value when partitioning the first i nodes into j segments, with transitions recorded in the predecessor matrix $pre[i][j]$. The final loop traces back from the last segment's optimal value to reconstruct the partition indices by following pre entries iteratively.

Algorithm 8: Full Training Pipeline

Input: Graph $G = (V, E, W, o)$, target partition number P_{max} , target ring partition number P_c

Output: Next partition a

$P \leftarrow \{V\}$;
 $samples \leftarrow \{\}$;

while not converge do

// perform P_{max} steps to generate partition and save into samples **for** i from 1 to P_{max} **do**

if $|P| \leq P_c$ **then**

// do ring partition

$G_l \leftarrow \text{GraphToLine}(G)$;
 $Emb \leftarrow \text{WRTWithRing}(G_l, P)$;
 $p, critic \leftarrow \text{PPO}(Emb)$;
 $a \leftarrow$ sample action from p ;
 $r \leftarrow$ radius of $G_l.V[action]$;
 $P' \leftarrow$ partition p by circle with radius r ;

else

// do wedge partition

$G_c \leftarrow \text{GraphToCircle}(G)$;
 $Emb \leftarrow \text{WRTWithWedge}(G_l, P)$;
 $p, critic \leftarrow \text{PPO}(Emb)$;
 $a \leftarrow$ sample action from p ;
 $angle \leftarrow$ angle of $G_l.V[action]$;
 $P' \leftarrow$ partition p by wedge with angle $angle$;

if $|P| = P_{max}$ **then**

$r \leftarrow \text{NormalizedCut}(G, P)$

else

$r \leftarrow 0$

$samples.add((G, P, p, critic, a, r))$;
 $P \leftarrow P'$

// calculate loss and train with samples ;

if $|samples| = target_size$ **then**

for $sample$ in $samples$ **do**

$p_{old}, c_{old}, r \leftarrow sample$ // here use sample as PPO input, in fact sample will do same as above to calculate p and critic.

$p, critic, critic' \leftarrow \text{PPO}(sample)$;
 $adv \leftarrow r - \gamma critic' + critic$;
 $loss_p \leftarrow \text{clip}(p/p_{old} * adv)$;
 $loss_v \leftarrow (r - \gamma critic' + critic)^2$;
 $loss_{ent} \leftarrow \text{Entropy}(p)$;
 $L \leftarrow w_p loss_p + w_v loss_v + w_{ent} loss_{ent}$;
;

Backward loss L ;

$samples \leftarrow \{\}$

Algorithm 9: Dynamic Programming for Ring Partition

Input: Precomputed cut weight matrix Cut , volume matrix $Volume$, number of partitions k

Output: Optimal Normalized Cut res , partition indices P

$sector_nc[i, j] \leftarrow (Cut[i] + Cut[j])/Volume[i, j]$
for all i, j ;

// $dp[i, j]$ means the best result when we perform partition on node i and it is the j -th partition

$dp[i, j] \leftarrow \infty$ for all i, j ;

$dp[0, 0] \leftarrow 0$;

// $pre[i, j]$ records where the value for $dp[i, j]$ transits from

$pre[i, j] \leftarrow 0$;

for i from 1 to $|Cut| - 1$ **do**

for j from 1 to $k - 1$ **do**

 // enumerate all $p < i$ and assume last partition is from p to i

for p from 1 to $i - 1$ **do**

$agg_res[p] \leftarrow \max(dp[p, j - 1], sector_nc[p, i]);$

$pre[i, j] \leftarrow \arg \min(agg_res);$

$dp[i, j] \leftarrow agg_res[argmin];$

// The last partition should be from p to $|Cut|$, update it to $dp[p, k - 1]$

for p from 1 to $|Cut| - 1$ **do**

$dp[p, k - 1] =$

$\max(dp[p, k - 1], sector_nc[p, |Cut| - 1]);$

$result \leftarrow dp[res_x, res_y];$

// get final partition indices

$r_x \leftarrow \arg \min(dp[:, k - 1]);$

$r_y \leftarrow k - 1$;

$P \leftarrow \{\}$;

while $r_y > 0$ **do**

$P \leftarrow P \cup \{r_x\};$

$r_x \leftarrow pre[r_x, r_y];$

$r_y \leftarrow r_y - 1$;

return $result, P$
